Electric Power Systems Research 231 (2024) 110334

Contents lists available at ScienceDirect

Electric Power Systems Research

journal homepage: www.elsevier.com/locate/epsr

Oppositional based artificial rabbits optimization applied for optimal allocation of nonlinear DG in distribution networks considering total harmonic distortion limit

Anamika Ghorai [a,*], Barun Mandal [b], Provas Kumar Roy [b], Chandan Paul [c]

[a] Department of Electrical Engineering, Adyapeath Annada Polytechnic College, Dakhineswar, West Bengal, India
[b] Department of Electrical Engineering, Kalyani Government Engineering College, Kalyani, West Bengal, India
[c] Department of Electrical Engineering, Dr. B C Roy Engineering College, West Bengal, India

ARTICLE INFO

Keywords:
Oppositional-based artificial rabbits optimization (OARO)
Nonlinear DG (NLDG)
Total harmonic distortion (THD)
Active power loss (APL)
Voltage deviation (VD)
Voltage stability index (VSI)
Type of DG

ABSTRACT

This paper proposes a new optimization approach to identify the optimal placement and sizes of distributed generation (DG) units in a radial distribution network (RDN). Inverter-based DG also known as nonlinear DG (NLDG) units inject nonlinear current into the system, which can cause harmonic distortion. This harmonic distortion can limit the penetration of DG in the system by affecting the stability and reliability of the power system. Therefore, it is essential to consider harmonic distortion when identifying the optimal placement and sizes of DG units in RDNs to ensure DG's safe and effective integration into the power system. The aim of the proposed work is to minimize real power loss, voltage deviation (VD), and total harmonic distortion limit (THD), and improve the voltage stability index (VSI) by integrating the search strategies of opposition-based learning and artificial rabbits optimization (ARO) to achieve better performance. The proposed algorithm, called opposition-based artificial rabbits optimization (OARO), considers different types of DG units like DG TYPE I and DG TYPE III and is suggested for two familiar RDNs: IEEE 33-bus, and 118-bus systems. The Pareto optimality concept has been introduced to solve the multi-objective problems of the systems. The simulation outcomes have been analyzed by comparing several optimization techniques in various cases. OARO has been shown to produce high-quality results with minimal iterations, reducing the time needed to solve the issue and conserving energy. Overall, the proposed approach offers a promising solution for identifying DG units' optimal placement and sizes in RDNs while considering various operating scenarios.

1. Introduction

The power sector is currently facing numerous challenges due to the increasing energy demand caused by modern lifestyles and the limitations of fossil fuel sources. One of the main challenges in the distribution system is minimizing transmission and distribution losses. Voltage instability becomes more prevalent day by day. However, the concept of "distributed generation" has emerged as a solution to these challenges. U.S. Department of Energy (DOE) says that DG is the modular electric generation or storage with control technologies that is connected near the point of use. DG unit's power output generally varies from a few kilowatts to a few megawatts [1]. A distribution generator (DG) can be defined as "a small-scale electric power generation unit that is installed 'behind the meter', typically at the end-of-use customers' premises and operated for totally or partially supplying the load" [2]. Distributed generation is a sustainable development practice. DG systems may be renewable like thermal–solar power and photovoltaic systems, fuel cells, microturbines, wind turbines, and storage systems, or non-renewable like combustion engines/generator sets. Depending on the DG source, it can generate alternating current (AC) from a synchronous or induction generator and direct current (DC) from a photovoltaic cell. It is not possible to connect a DC or variable AC generator immediately to the AC distribution system. It is connected through a power electronics interface. So, DG can be connected to the system directly or through the inverter [3]. The central generation (CG) system of the early days was a centrally stationed power plant used to generate bulk power to be transmitted through transmission and distribution lines. But in the DG-connected system, power is generated near the consumer site. Therefore, there is a probability that the voltage level, power quality, reliability, power losses, protection, and safety will have an effect across the entire distribution system [4]. Therefore, choosing the optimum position & size of DGs can mitigate various problems, namely, lowering APL and enhancing the voltage profile, system

* Corresponding author.
E-mail address: phdanamika@gmail.com (A. Ghorai).

https://doi.org/10.1016/j.epsr.2024.110334
Received 11 June 2023; Received in revised form 15 January 2024; Accepted 16 March 2024
Available online 23 March 2024

Nomenclature

DG	Distributed generator
OARO	Oppositional based ARO
RDN	Radial distribution network
APL	Active power loss
OPDG	Optimal planning of distributed generators
BCBV	Branch current to the bus voltage
I_i^{DG}	Fundamental Current provided by DG
Q_i^{DG}	Fundamental reactive power provided by DG
$I_i^{DG(h)}$	hth Order harmonic current injected by NLDG
I_{br}	Branch current of brth Branch
N_{branch}	Total number of branches of the RDN
X_{mn}	Reactance of the line connecting buses m and n
S_n	Apparent power of bus n
Q_n	Reactive power of bus n
$v_{i,h}$	hth Harmonic voltage at bus i.
$V_i^{\min}$, $V_i^{\max}$	Lower limit and Upper limit of voltage at bus i
$P_{DG}^{\min}$, $P_{DG}^{\max}$	Minimum and maximum input active power of DG
S_i^{DG}	Apparent power of ith unit
$pf_{DG}^{\max}$, $pf_{DG}^{\min}$	Maximum and Minimum power factor limit of DG
U, L	Upper and lower bound of a variable
dim	The size of optimization problem
$X_{i,j}^{o}$	Opposite point
$X_{i,k}^{new}$	The artificial rabbit's new population
m_{fi}	Fuzzy membership function
ARO	Artificial Rabbits Optimization Algorithm
NLDG	Nonlinear DG
THD	Total harmonic distortion
VSI	Voltage stability index
BIBC	Bus injection to branch current
P_L	Active power loss
P_i^{DG}	Fundamental active power provided by DG
V_i	Fundamental voltage at bus i
R_{br}	Resistance of the branch
PL_b	Base power loss of the RDN
R_{mn}	Resistance of the line connecting buses m and n
z_{mn}	Impedance of the line connecting buses m and n
P_n	Active power of bus n
$v_i^{(1)}$	The fundamental voltage at bus i
THD_i	Total voltage harmonic distortion at bus i
N_{BUS}	No of buses in a RDN
N_{DG}	The total no of DG
$pf_{DG,i}$	Power factor of ith unit of DG
$Maxit$	Maximum iteration
$X_{i,j}$	Initial population of organisms
$popsize$	The size of the population of organisms
A	Energy factor
L	Speed during detour foraging
M_k	Normalized membership function of Kth solution

stability, reliability, and performance. Maximum research work focuses on the allocation of DG to reduce transmission loss [5]. Enhancing the integration of various DG in the RDN specifically the renewable DGs like PV and wind generation sources has become a main objective of the distribution system for its many technical, environmental, and economic merits. This type of source is connected through inverters injecting harmonics into the system. This inverter is the leading source of harmonics. So, inverter-based DG introduces harmonics into the system. This type of DG is described as a nonlinear DG (NLDG). The individual harmonics distortion in voltage (IHDv), along with the total harmonic distortion in voltage (THDv) in RDNs, has been increased due to this type of DG [6]. So, maintaining the power quality of a distribution system becomes one of the important challenges. As per IEEE Standard 519, THDv and IHDv must be lower than 5% and 3%, respectively [7]. Harmonic load flow studies are most important to analyze the presence of harmonics in the network.

Identifying the optimum location & size of DG has engrossed huge interest from researchers to get maximum benefits on the distribution system. Different optimization techniques have been continuously designed and carried out to resolve the DG placement problems efficiently. Different types of techniques namely analytical approaches, numerical methods, meta-heuristic algorithms, ANN algorithms, and hybrid algorithms, etc have been used in different optimization problems [8]. Metaheuristic optimization techniques have been applied to numerous optimization problems of different disciplines. Compared to other optimization methods, it executes faster. Many Metaheuristic optimization techniques like Genetic Algorithm (GA), Particle Swarm Optimization (PSO), Water Cycle Algorithm (WCA), Tabu Search (TS), Honey Bee Algorithm (HBA), Ant Colony Optimizer (ACO), Ant Lion Optimization algorithm (ALOA) and Grey Wolf Optimizer (GWO), etc algorithms have been employed for optimal allocation of DG [9]. A number of studies have been carried out to minimize the active power loss of the system by optimizing DG size and position in the network using different approaches. The loss sensitivity factor (LSF) was applied to find out the candidate bus and decreased the state space. After that, an algorithm was applied to find the optimum position and size of the DG to minimize the active power loss (APL) as a single objective function for single or multiple DG placement problems. To determine the best positioning and size of the DG and capacitor bank moth flame optimization (MFO) & Sine Cosine Algorithm (SCA) was proposed in [10]. In another study, QOCSOS (quasi-oppositional chaotic symbiotic organisms search) algorithm was applied for searching the optimum number, positions, and power factor of DG units to reduce the active power loss of IEEE 33, 69, and 118-bus RDNs [11]. Teaching-learning-based optimization (TLBO),& quasi oppositional TLBO (QOTLBO) [12] was implemented to determine the optimal bus for DG connection and sizes of DG units in RDNs to reduce the APL and VD and improve the VSI. Combining GA and PSO together (GA/PSO) [13], and quasi-oppositional swine influenza model-based optimization with quarantine (QOSIMBO-Q) [14] was introduced to solve the same objective function. Kansal, S et al. proposed a methodology introducing a multi-objective function to determine the optimum location and optimal power factor for DG, and the best location for DGs using particle swarm optimization (PSO) [15]. For identifying the optimum DG placement in the distribution network while incorporating single and multi-objective functions, comprehensive TLBO (CTLBO), another enhanced variation of TLBO, was proposed in [16]. Maximum research work was done on IEEE 33 and IEEE 69 radial networks. A chaotic artificial flora optimization technique was designed to find the optimal allocation and capacity of DGs (CAFO-OPSDG) to regulate the voltage of the network in specified limits and reduce the APL in research work. The fitness function of the CAFO-OPSDG algorithm included power loss minimization, voltage regulation, and penalty cost [17]. In some studies, different types of DG have been considered. The honey badger algorithm (HBA) was proposed for identifying the best location in the network and size for capacitors and various DG types (DG TYPE-I and DG TYPE-III) to reduce the network's overall active power loss [18]. In [19], a single fitness function combining two objective functions introducing a weighted sum method was presented for the optimal allocation of several DG units in the IEEE 69-bus network. Minimization of VD and reactive power loss was considered for the objective

function. The optimal solution has been achieved using grey wolf optimization (GWO). The quasi-oppositional differential evolution Lévy flights algorithm (QODELFA) was introduced in another study to carry out the optimal planning of distributed generators (OPDG) problem in radial distribution networks (RDNs). The minimization of active power loss, the voltage profile improvement, and the enhancement of the voltage stability index were considered objective functions [20]. Manta-ray foraging optimization algorithm (MRFO) was applied in [21] for the same objective function. Using LSF and the ant lion optimization algorithm (ALOA), the best placements and capacity of Photovoltaic (PV) and wind turbine-connected DG sources were identified in networks. This multi-objective function included minimizing overall power losses, enhancing voltage profiles, and the VSI of RDNs in [22]. The appropriate positioning of DG sources in distribution networks was explored using the chaotic symbiotic organisms search (CSOS), which aims to minimize real power loss and raise voltage stability in [23]. In another research work [24] a multi-objective opposition-based chaotic differential evolution (MOCDE) algorithm was addressed to attain the OPDG problem for solving multi-objective. The objectives of this study were embedded in maximizing economic benefits, minimizing power loss, and minimizing voltage deviation. To find the appropriate capacity and position of distributed generation photovoltaic (DGPV), multi-objective chaotic mutation immune evolutionary programming (MOCMIEP) was implemented to decrease. Fast Voltage Stability Index (FVSI) and APL concurrently in [25]. In the above research work, the harmonic limit for the inverter interfaced distribution generation (IIDG) is not considered a constraint. IIDG can increase the harmonic level of the network. Abbas, Ahmed S et al. introduced the biogeography-based optimization (BBO) algorithm to find optimal sitting and sizing of inverter-based DGs and capacitors and compared the result with particle swarm optimization (PSO) and Genetic Algorithm (GA). Active and reactive loss reduction, a decrease in the amount of transmission line energy purchased, and an improvement to the voltage profile were included in the objective function considering equal and unequal constraints. According to IEEE 519 standard, the total harmonic distortion (THD) constraint was also included in the objective function. It is one of the main advantages of this work [26]. In another study, four single objective functions were proposed to minimize the power loss, THD, and the capacity of PVDG units, and enhance the voltage profile. Different constraints were considered to meet the IEEE 519 standard. Proposed improvements were implemented for IEEE 69-bus & IEEE 33-bus in [27] A comprehensive study was made on the optimal placement of solar PV-DG in the Radial Distributed Network to decrease network losses and % THD of bus and improve the voltage profile. A multi-objective function was proposed to identify the optimal location and optimal size of solar PV-DG using PSO algorithm [28]. Eid et al. in their recent endeavor suggested the Bonobo optimization approach [29] for solving the multi-objective DG integrated OPF problem of distribution systems. Furthermore, Archimedes optimization algorithm [30] was proposed by Eid et al. for locating RDN in distribution systems. In many research studies, the weight factors are determined as part of the index optimization process using the integrated multi-objective optimization (IMO) framework [31,32] rather than being assumed or left to the decision maker's preferences. With the help of this method, the best sites and dimensions for wind turbine generators (WTGs) and superconducting magnetic energy storage systems (SMESs) are determined. Reducing power loss and enhancing the voltage of the network should be key objectives to improve the efficacy of a transmission system. Numerous research works developed by adding certain objective functions apart from APL minimization and voltage stability. The most commonly identified objective functions are reactive power loss, operational cost, investment cost, voltage stability index, and THD, among many others. [33,34]. A newly innovated bio-inspired meta-heuristic method called artificial rabbits optimization (ARO) has been introduced and comprehensively evaluated in this study. The ARO algorithm is inspired by the survival techniques used by rabbits in the wild, such as detour foraging and random hiding [35]. After that, a modified version of ARO *i.e.* oppositional-based ARO (OARO) has been applied to optimize the multi-objective problem. For the objective function formulation of the OPDG problem, APL and VD reduction, and VSI improvement are included in the maximum approach. THD is one of the most important constraints for inverter-based DG or NLDG that is not included in previous studies. Therefore, this inspires us to comprise a new objective function *i.e.* THD minimization on the existing system considering the IEEE 519 standard. The new method has been developed to find the optimal position and size of DG in RDNs by considering four objectives. It aims to reduce active power loss (APL), voltage deviation (VD), and total harmonic distortion (THD), and enhance the voltage stability index (VSI). The study is based on mainly two types of DGs (TYPE-I, TYPE-III). The algorithm has been tested on IEEE 33-bus and 118-bus RDNs, and comparisons have been conducted with numerous other past approaches mentioned above research work.

1.1. Contributions

The following summarizes the significant contributions of this work:

(a) The OARO is proposed to solve the OPDG problem, considering two types of DG units: DG TYPE I with unity power factor (UPF), and DG TYPE III with 0.866 lagging and an optimum power factor (OPF).
(b) Here, a multi-objective function has been designed to enhance the DG penetration including loss minimization, enhancement of voltage deviation, voltage stability index improvement, and total harmonic distortion reduction.
(c) NLDGs are the source of harmonic distortion. Harmonic power flow is included within the optimization framework to calculate THD. The inclusion of THD is one of the new objectives of the OPDG problem.
(d) Three case studies are conducted to evaluate the effectiveness of the proposed method. Case Study 1 considers APL minimization, Case Study 2 focuses on the simultaneous reduction of APL, VD, and improvement of VSI, while Case Study 3 considers APL and THD minimization.
(e) The Pareto-optimal solutions have been found for case studies 2 and 3. The weighting factors are not presumptive or subject to the decision-maker's own choices.
(f) The outcome of the suggested OARO method has been compared with the outcomes from the original ARO and other published optimization algorithms.

2. Problem formulation

2.1. DG type

The following four categories [36] can be used to describe the distributed generators

TYPE-I: Only injects real power into the network *i.e.* power factor unity, such as photovoltaic cells (PVs).

TYPE-II: Operating at zero leading power factor& producing reactive power like the capacitor

TYPE-III: Add both active & reactive power into the network, such as the doubly-fed induction generators seen in wind turbines.

TYPE-IV: Introduce real power & consume reactive power, like the wind turbine's squirrel cage induction generators.

In this study, TYPE I and TYPE III DGs are taken into consideration. Fixed power factor (0.866 lag) and optimum power factors are considered for TYPE III DG. Maximum DGs are connected to the distributed network through an inverter or converter. so, harmonics are introduced to the system. A harmonic power flow analysis has been performed for this.

2.2. Harmonic power flow analysis

This is a technique for estimating harmonics in the system, harmonic power flow is helpful when a nonlinear device is present in the system. In this study, harmonic load flow based on network topology is applied [37] wherein two matrices, namely BIBC and BCBV, are constructed. After that, the optimization algorithm is connected with it. At every bus, THD is determined using harmonic load flow. For this, DG modeling is completed initially.

2.3. DG modeling

DG can act as a constant current source and supply harmonics to the system. Fundamental current can be found out from the power rating of the DG as per Eq. (1) [38].

$$I_i^{DG} = \left[\frac{P_i^{DG} + jQ_i^{DG}}{V_i}\right]^* \tag{1}$$

The following formula (2) can be used to compute the DG's harmonic current contribution.

$$I_i^{DG(h)} = k^{(h)} I_i^{DG} \tag{2}$$

Where, P_i^{DG}, Q_i^{DG} are considered as fundamental active and reactive power generation by DG units connected at bus i, I_i^{DG} is fundamental current supplied at bus i by NLDG units, V_i presents fundamental voltage at bus i, $I_i^{DG(h)}$ is the h th order harmonic current injected by NLDG. This $k^{(h)}$ can be obtained from Table 2 specified in IEEE 519 standard [39]

2.4. Objective functions

2.4.1. Minimization of active power loss

In a simple radial distribution system, the mathematical formula for the objective function of reducing active power loss (P_L) throughout distribution networks is as follows:

$$OF_1 = \min\left(\frac{P_L}{PL_b}\right) \quad \text{where} \quad P_L = \sum_{br=1}^{N_{branch}} R_{br} I_{br}^2 \tag{3}$$

Where, R_{br}, and I_{br} represent the branch resistance & the branch current of brth branch respectively; N_{branch} represents the total number of branches of a distribution network, the base power system loss is denoted by PL_b [40,41].

2.4.2. Improvement of voltage deviation

Improving the voltage profile is one of the targets of appropriate placement and sizing of DGs. The voltage deviations must be reduced. The objective function of reducing voltage deviations can be described as follows:

$$OF_2 = \min\left|\frac{\text{VD}}{VD_{base}}\right| \quad Where,\ VD = \frac{\sum_{i=1}^{n}\left(V_{nom} - V_i\right)^2}{V_{nom}} \tag{4}$$

Where V_i represents the ith bus voltage and n is the number of buses present in the RDS. V_{nom} is rated voltage. $V_{nom} = 1$ p.u. Furthermore, in numerous research papers, total voltage deviation (TVD) is formulated as [40]:

$$TVD = \sum_{i=1}^{n}\left(1 - V_i\right) \tag{5}$$

However, in this study, Eq. (4) is used to describe the objective function for improving the voltage profile [42]:

2.4.3. Improvement of voltage stability index

Maintaining the voltage stability index (VSI) within a specified range is essential for improving the voltage level of the distribution system under heavily loaded conditions. The $VSI\,(n)$ of bus n of a radial distribution system is defined by [42]:

$$VSI\,(n) = \left|V_m\right|^4 - 4\left[P_n R_{mn} + Q_n X_{mn}\right]\left|V_m\right|^2 + 4\left[P_n R_{mn} - Q_n X_{mn}\right]^2 \tag{6}$$

Where, $R_{mn}\&X_{mn}$ denote the resistance and reactance of the line connecting buses m and n respectively. VSI_{base} denotes the base case voltage VSI. So, using the formula (7), maximizing the VSI becomes minimization.

$$\max\left(VSI(n)\right) = \min\left(\frac{1}{VSI\,(n)}\right) \tag{7}$$

In many research papers, VSI has been introduced as [41]

$$VSI\,(n) = 1 - \left[2\left(P_n R_{mn} + Q_n X_{mn}\right) - V_n^2\right]^2 - 4S_n^2 Z_{mn}^2 \tag{8}$$

In this study, Eq. (6) has been used for the calculation of VSI. The objective function for enhancing the voltage stability index is taken from [42],

$$OF_3 = \min\left|\frac{VSI_{base}}{VSI\,(n)}\right| \tag{9}$$

2.4.4. Minimization of average total harmonic distortion

NLDG units are the origin of harmonic distortion. Which is restricted to the DG penetration level. So, proper allocation of the position and size of DG is required to minimize the average harmonic distortion. Total voltage harmonic distortion (THD_i) at bus i as follows:

$$THD_i(\%) = \frac{\sqrt{\sum_{h=2}^{h_{\max}}\left|v_{i,h}\right|^2}}{v_i^{(1)}} \times 100\% \tag{10}$$

5% is often specified as the maximum allowable THD per IEEE 519 standards [43]. So the average THD_v is another objective in case of NLDG

$$OF_4 = THD_v = \min\left(\frac{\sum_{i=1}^{N_{BUS}}\left|THD_i\right|}{n}\right) \tag{11}$$

Case study 1 (APL minimization [11]):

$$F_1 = \min(OF_1) \tag{12}$$

Case study 2 (Simultaneous APL and VD minimization, as well as VSI enhancement):

$$F_2 = \min(W_1 \times OF_1 + W_2 \times OF_2 + W_3 \times OF_3) \quad \text{where } W_1 + W_2 + W_3 = 1 \tag{13}$$

The weighting factors, W_1, W_2 and W_3 have values between (0, 1) that is adjusted uniformly [44].

Case study 3 (Simultaneous minimization of APL and THD):

$$F_3 = \min\left(W_1 \times OF_1 + (1 - W_1) \times OF_4\right) \tag{14}$$

The weighting factor, W_1 has a value between (0, 1) that adjusts uniformly. At first, $W_1 = 0$ is chosen, and then adjustment has been made in the intervals of 0.05–1.

2.5. System constraints

2.5.1. Equality constraint

The power balance equation for active and reactive powers in the network should be shown by the following equations: Where

$$P_{SLACK} + \sum_{m=1}^{N_{DG}} P_m^{DG} = \sum_{n=1}^{N_{BUS}} P_{LOAD,n} + \sum_{k=1}^{N_{branch}} P_{LOSS,K} \tag{15}$$

$$Q_{SLACK} + \sum_{m=1}^{N_{DG}} Q_m^{DG} = \sum_{n=1}^{N_{BUS}} Q_{LOAD,n} + \sum_{k=1}^{N_{branch}} Q_{LOSS,K} \tag{16}$$

Where, P_{SLACK} and Q_{SLACK} represent active and reactive powers provided by the slack bus, respectively; P_m^{DG} and Q_m^{DG} are the generated active and reactive power outputs of the mth DG unit, respectively; $P_{LOAD,n}$ and $Q_{LOAD,n}$ are active and reactive load demands at the nth bus, respectively; $P_{LOSS,K}$ and $Q_{LOSS,K}$ represent the kth branch's active and reactive power losses, respectively.

2.5.2. Inequality constraints

- Bus voltage constraints: The bus voltage must be controlled in the definite range. $V_i^{\min}$&$V_i^{\max}$ of bus voltage are normally 0.95 & 1.05 per unit, respectively. Bus voltage of ith bus is represented using (17)

$$V_i^{\min} \le V_i \le V_i^{\max}, i = 1, \dots, n \tag{17}$$

- DG sizing limits: Following Equation suggests that input of the distributed generators' active powers P_i^{DG} from ith unit must be within a specified range (18)

$$P_{DG}^{\min} \le P_i^{DG} \le P_{DG}^{\max}, i = 1, \dots, N_{DG} \tag{18}$$

Reactive power (Q_i^{DG}) and apparent power (S_i^{DG}) of ith unit can be calculated by using Eq. (19)

$$S_i^{DG} = \frac{P_i^{DG}}{pf_{DG,i}} \quad and \quad Q_i^{DG} = S_i^{DG} \times \sin\left(\cos^{-1} pf_{DG,i}\right) \tag{19}$$

- Power factor limit of DG: DG units can be employed within $pf_{DG}^{\max}$&$pf_{DG}^{\min}$ power factor ranges.

$$pf_{DG}^{\min} \le pf_{DG,i} \le pf_{DG}^{\max}, i = 1, \dots, N_{DG} \tag{20}$$

- Limitations on individual voltage harmonic distortion: The IEEE-519 standard also fixes limitations on individual voltage harmonic distortion for each bus.

$$IHD_i(\%) = \frac{v_{i,h}}{v_i^{(1)}} \times 100\% \le 3\% \text{ [43]} \tag{21}$$

3. OARO algorithm

The OARO algorithm is a modified version of the original ARO algorithm that incorporates opposition-based optimization (OBO) strategies. The OBO method in OARO enables the algorithm to search over a more effective search area and produce a superior outcome. Consequently, the algorithms' ability to explore is improved.

3.1. Opposition-based optimization (OBO)

The calculation of the opposite point in detail is represented as follows: Firstly, the initial population of organisms is calculated randomly within the specified boundary according to Eq. (22)

$$X_{i,j} = L_j + rand(0,1) \times (U_j - L_j) \quad j = 1, 2, \dots, dim; \quad i = 1, 2, \dots, popsize \tag{22}$$

Where, L: lower bounds of a variable; U: Upper bounds of a variable. dim: The size of optimization problem; $Popsize$: The size of the population of organisms according to the opposition point definition, the new opposite point to the point can be determined as follows [45]

$$X^o{}_{i,j} = L_j + U_j - X_{i,j} \tag{23}$$

Now, if $f(X)$ is considered as a fitness function then first calculate $f(X_{i,j})$ and $f(X^o{}_{i,j})$. If $f(X^o{}_{i,j}) \le f(X_{i,j})$, then $X_{i,j}$ can be changed with $X^o{}_{i,j}$; otherwise we carry on with $X_{i,j}$. In order to proceed with the more appropriate one, the initial point and its opposing point are considered and analyzed simultaneously.

3.2. ARO algorithm

Two laws of rabbit survival are considered for the planning of the ARO algorithm. These are detour foraging and random hiding. Detour foraging is a searching approach to prevent natural predators from detecting them by feeding the grass to rabbits near the nest. Random hiding is an approach in which rabbits move to other terriers, mostly to hide further away. By applying the following equations, a new population is created from the initial population. For this first calculated the energy factor. The energy of the rabbits is used by ARO to create a search scheme since it depletes with time, reflecting the change from exploration to exploitation. The energy factor in the algorithm for artificial rabbits is defined as follows [35]:

$$\mathrm{A} = 2 \times \log\left(\frac{1}{rand_3}\right) \times th \quad \text{Where, } th = 2 \times \left(\frac{1 - \mathrm{It}}{\mathrm{MaxIt}}\right) \tag{24}$$

It: current iteration $MaxIt$: maximum iteration if A is greater than 1, the detour foraging method is applied using Eqs. (25)–(27) to determine the new position of the rabbits. The equations are described below.

$$X_{i,k}^{new} = X_{j,k} + R \times \left(X_{i,k} - X_{j,k}\right) + \mathrm{round}\left(0.5\left(0.05 + \mathrm{rand}_1\right)\right) \times n_1 \tag{25}$$

$$R = \mathrm{L} \times C, \quad L = \left(e - e^{\left(\frac{It-1}{MaxIt}\right)^2}\right) \times (\sin(2)\pi \times rand(0,1)) \quad \text{and}$$

$$G = randperm(\dim) \tag{26}$$

$$C(n) = \begin{cases} 1 & if\ n == G(l) \\ 0 & else \end{cases} \quad l = 1, \dots, [rand_3, dim] \tag{27}$$

where, $X_{i,k}^{new}$: indicates the artificial rabbit's new position. $X_{i,k}$: indicates the artificial rabbit's at ith position. $X_{j,k}$: represents the random artificial rabbit's position. The stochastic numbers $rand_1$, $rand_2$ and $rand_3$ range from 0 to 1. The running length is denoted by L which is the moving speed during detour foraging. n_1 follows the conventional normal distribution. The random number n_1 from the normal distribution primarily reflects the perturbation. ARO can perform a global search and avoid local extremes by perturbing the final term of Eq. (25). if A is less than 1. the random hiding method is used to determine the new position of the rabbit's applying the Eqs. (28) to (31).

$$X_{i,k}^{new} = X_{i,k} + \mathrm{R} \times \left(rand_4 \times \mathrm{b}_{i,k} \text{-} X_{i,k}\right) \tag{28}$$

$$\mathrm{H} = \left(\frac{\mathrm{MaxIt} - \mathrm{It} + 1}{\mathrm{MaxIt}}\right) \cdot \mathrm{n}_2 \tag{29}$$

$$\mathrm{b}_{i,k} = X_{i,k} + \mathrm{H} \times Gr \times X_{i,k} \tag{30}$$

$$Gr(t) = \begin{cases} 1 & \text{if } t = \lceil rand_5 \times \dim \rceil \\ 0 & \text{else} \end{cases} \quad \text{where} \quad t = 1, \dots, \dim \tag{31}$$

where $i = 1, \dots,$ popsize and $k = 1, \dots, dim$ and The typical normal distribution is followed by n_2 With stochastic perturbations, the hidden parameter H falls linearly from 1 to $\frac{1}{MaxIT}$. $b_{i,k}$ signifies a randomly chosen burrow among the d burrows developed by the rabbit at random for hiding, and $rand_4$ and $rand_5$ stand for the random integer we choose between 0 and 1. In this way, a random hiding method is performed to generate a new position for the rabbit. The fitness value is evaluated for each individual and modified the position to find the best position

pseudo-code of the ARO algorithm is provided below:

- Forming the optimization problem and selecting the constraints.
- Include control parameters, the maximum number of iterations (MaxIT), and the total number of populations (Popsize).
- Calculating the fitness function after randomly initializing a group of rabbits

• Identify the best rabbits.

for iter = 1: MaxIT **do**
  for i = 1: popsize **do**
    Use (24) to determine the energy factor A.
    if A > 1 **then**
      Randomly selects one rabbit from the initial rabbit's position.
      Applying (26)–(27), compute R.
      Apply the detour foraging method to find a new rabbit position using (25).
      Determine fitness value $f(x_i)$, for the new rabbit's position (x_i).
      Update the new rabbit's positions if fitness is better.
    else
      Create b burrows and choose one at random using (29)–(31).
      Apply the random hiding technique using (28).
      Determine fitness value $f(x_i)$, for the new rabbit's position (x_i)
      Update the new rabbit's positions if fitness is better.
    end if
  end for
  Identify the best artificial rabbit.
end for
Output the most appropriate artificial rabbit.

4. Implementation of OARO to optimal placement and size of DG

This section provides detailed steps to minimize the APL, VD, and THD while maximizing the VSI in order to execute the OPDG problem in RDNs using OARO algorithm.

Step 1: Input the bus and line data of RDNs system, the DG type, DG number, and other constraining parameters.

Step 2: Run the power flow algorithm to obtain the base values of RDNs.

Step 3: Initially, a random population is generated for the OPDG problem by evenly dispersed control variables between upper and lower boundaries of DG size, power factor & location (bus no).

Step 4: Implement conventional power flow for each individual population to obtain the active power loss, voltage deviation and voltage stability index.

Step 5: Run harmonic power flow to calculate the total harmonic distortion (THD) of the system due to the presence of DG. For this, first calculate the harmonic current injected into the system considering the inverter-based DG harmonic spectrum using (1) and (2). Then calculate the harmonic voltage component.

Step 6: If any system limitation is violated, the particular population is discarded, and the procedure is repeated until the required number of populations are formed. In the suggested OARO algorithm, the opposite population is created using the OBL methodology as described in (22) and (23).

Step 7: Determine the fitness value using (12) to (14). The final population is chosen against the initial population and opposed based on population size.

Step 8: Calculate new populations using the ARO algorithm and determine the objective function by repeating the step 4 to step 7 and updating the population depending on the fittest one. If the maximum number of iterations is achieved for single-objective optimization described in (12), the iterative process should be stopped; otherwise, continue steps 4 to 7. Remain the outcomes in an array (also referred to as the Pareto-optimal set described in [14]) and stop for multi-objective optimization (described in (13) & (14)) issues if the current iteration is higher than or equal to the maximum iteration; otherwise, continue steps 3 to 7 until the problem is solved.

Step 9: When solving the bi-objective problem according to Eq. (13), increase the value of W_1 in steps of 0.05 and go back to step 3 until step 8. Continue doing this until the value of W_1 approaches 1. When doing a tri-objective (14), optimization using the three weighting factors increases the value of each weighting component in increments of 0.1 starting at 0 and going up to 1, so that the sum of W_1, W_2 and W_3 equals 1, and then repeat step 3 through step 8 each time.

Step 10: The procedure outlined above produces the Pareto-optimal solutions, which are a non-dominated set of responses. The suggested approach uses a fuzzy-based mechanism to select the optimal compromise solution from the Pareto front when addressing multi-objective optimization problems. The fuzzy membership function (m_{fi}) and the normalized membership function M_k for each non-dominated solution k are determined by applying the fuzzy logic theory to each objective function in the manner described below:

$$m_{fi} = \begin{Bmatrix} 0 & m_i <= 0 \\ m_i & 0 < m_i < 1 \\ 1 & m_i >= 1 \end{Bmatrix} \; where \; m_i = \frac{OF_i^{\max} - OF_i}{OF_i^{\max} - OF_i^{\min}} \quad (32)$$

$$M_k = \frac{\sum_{i=1}^{n} m_{fi}^k}{\sum_{k=1}^{o}\sum_{i=1}^{n} m_{fi}^k} \text{ where}$$
$$M_k = \text{ the normalized membership function of } K\text{th solution,} \quad (33)$$

OF_i = ith objective function, OF_i^{max}, OF_i^{min} = maximum and minimum value of ith objective function respectively n&o represent no of objective function and the number of non-dominated solutions respectively. The optimal non-dominated solution can be identified when Eq. (33) is maximum, and all objectives have the highest normalized sum of membership function values. The process is finished, and the optimal solution to the optimization problem has been found.

Step 11: Find the best population.

Step 12: Go to step 13 if the termination requirement has been fulfilled.

Step 13: Display the final results and record the outcomes

5. Results & discussions

The OARO and ARO has been tested on two test systems: The IEEE-33 bus, and 118-bus systems. The load flow has been executed using the backward–forward sweep algorithm, and THD and IHD are calculated using the harmonic power flow. The following two test networks are accounted for verifying the efficacy and reliability of the suggested approach. In case study 1, an initiative has been taken to reduce the APL of the system; case study 2 takes into account all three objectives to reduce the APL & VD while also enhancing the VSI; and case study 3

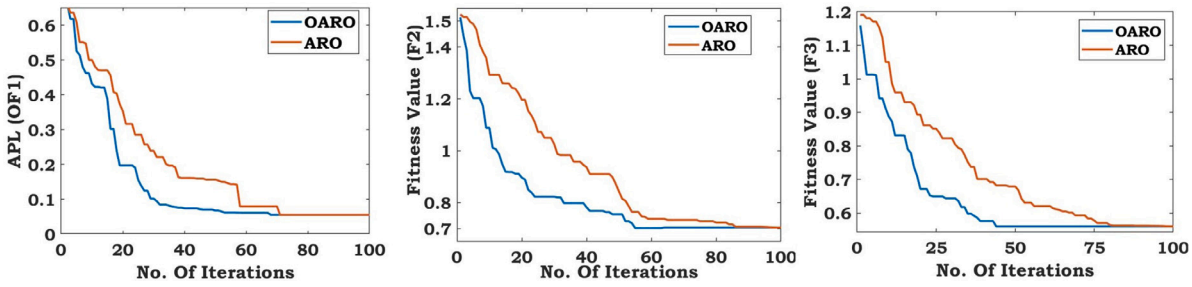

Fig. 1. Convergence characteristics for (a) Case Study 1 for DG TYPE III (OPF) of the 33-bus system (b) Case Study 2 for DG TYPE I (UPF) of the 118-bus system and (c) Case Study 3 for DG TYPE I (UPF) of the 118-bus system.

deals with the simultaneous reduction of THD and APL. Two distinct test systems, including DG type, are extensively analyzed for each scenario. These three types of DGs are DG TYPE I, DG TYPE III at fixed power factor (0.866 lag), and optimal power factor. The MATLAB R2021b platform has been used to code the algorithm. To find the optimal option, OARO & ARO conducted 20 independent tests for each test system. The original ARO approach is used to address the issue of result comparability. All test networks' initial data is provided in Table 1. Three DGs are installed for IEEE 33 bus system and seven DGs are installed for IEEE 118 bus system.

Table 1
Test networks' data.

Test network	33-bus	118-bus
Total load (MVA)	(3.715 + j2.300)	(22.709 + j17.041)
Active Power loss (KW)	210.988	1298.092
Minimum Voltage (p.u.)	0.904	0.869
Base voltage (KV)	12.66	11
Voltage deviation	0.133808	0.357641
VSI	0.6672	0.5697

5.1. RDS 1: IEEE 33-bus

5.1.1. Case study 1: Active power loss minimization

The minimization of Active Power Loss (APL) (F_1) is defined as an objective function in this case according to (12). The ARO & OARO algorithm is suggested for DG operating on UPF, 0.866 lagging, and OPF. Table 3 represents the list of the outcomes. 210.988 kW is the active power loss without DG. Using the suggested algorithm, it can be seen that the active power loss is decreased to 72.785 kW with DG TYPE I (Case 1.1). The result of OARO, ODELFA [20], and SFSA [42] are identical, as shown in Table 3, however, the total DG capacity is reduced to 2.9429 MW from 2.9467 MW and 2.9477 MW using OARO algorithm. The suggested OARO's total power loss is less than that of the krill herd algorithm [46], LSFSA [47] and QOSIMBO-Q [14], among others. The loss is reduced to 15.347 kW, the same as QODELFA, when DG operating at 0.866 lagging pf (Case 1.2), but the total DG capacity is decreased to 3.4621 MW from 3.4634 MW. The suggested method reduces active power loss to 11.740 kW by installing DG TYPE III with the best power factor (Case 1.3), which is better for QOCSOS [11] and SFSA [42]. This illustrated how significantly the power loss reduction is influenced by the optimal choice of power factor of DG units. Both the OARO and ARO algorithms consistently produced the same real power loss showing in results across all scenarios. However, as shown in Fig. 1(a) the convergence rates of OARO for better results are quicker than those of ARO in every scenario. The voltage profile of the 33-bus RDNs has been improved after the attachment of DG units, going from 0.904 (base case) to 0.9687 p.u., 0.9922 p.u., and 0.9922 p.u. for Cases 1.1–1.3, accordingly. It can be seen that the voltage profile of the network is greatly improved when the DG with power factor 0.866 lag (Case 1.2) and OPF (Case 1.3) have been implemented. For bus number 17, overall harmonic distortion is at its highest in all three cases. For Cases 1.1–1.3, the 33-bus test network's THD has been raised from 0 (base case) to 2.10%, 3.14%, and 3.13%, respectively for NLDG. However, it does not go above the permitted THD limit. This study also includes additional harmonic analysis.

5.1.2. Case study 2: Simultaneous APL and VD minimization, as well as VSI enhancement

The simultaneous minimization of APL (OF_1), VD (OF_2), and VSI^{-1} (OF_3) is analyzed in this scenario according to Eq. (13). The suggested OARO and ARO results are shown in Table 4 along with comparisons to the other approaches. Using OARO, the APL is reduced to 77.873 kW with unity power factor DGs (Case 2.1), which is significantly higher than the APL of 77.3793, 77.408 kW, and 77.410 kW using MRFO [21], QODELFA [20] and SFSA [42] respectively. Here, weighting factor has been varied uniformly and a Pareto optimal front is shown in Fig. 3 where others chose it randomly. However, the VD and VSI^{-1} (in p.u.) produced using the suggested algorithm is far better than those computed using the SFSA [42], MRFO [21], and QODELFA [20] algorithms. VD and VSI for UPF is 0.00598 p.u. and 0.9213 p.u. The APL and VD are decreased to 15.496 kW and 0.00035 p.u., respectively, while the VSI is improved to 0.9673 p.u. for Case 2.2. The APL and VD are reduced to 11.905 kW and 0.000338 p.u., respectively, while the VSI is enhanced to 0.96751 p.u. for Case 2.3. The OPF obtained by the OARO algorithm is 0.903, 0.894, and 0.719. Because of the lower power factor values, the system receives a considerably higher amount of reactive power. The voltage profile is greatly enhanced as a result. Compared to the previous three cases, The OARO gives a loss reduction that is almost 0.5 percent better than the Other method, VD is reduced to 0.000338, which is moderate to the other three algorithms, and VSI is also improved to 0.96751. The voltage profiles of the 33-bus network for four cases (without DG, With DG at unity pf, fixed pf, and optimal pf) are shown in Fig. 2(a). This can be seen in this diagram, the voltage magnitude at the buses is extremely close to the voltage's rated value (1.0 p.u.) for Case 2.3 & case 2.2. Case 2.3 has a considerably higher minimum voltage (0.994 p.u.) than case study 1 (0.9797 p.u.) & base case (0.904), which is an improvement. The 33-bus test network's THD is the maximum for bus no 17. It has been increased for Cases 2.1–2.3 from 0 (base case) to 2.47%, 3.23%, and 3.227%, respectively, for NLDG. However, It does not exceed the allowed THD limit.

5.1.3. Case study 3: Simultaneous minimization of APL and THD

In this scenario, both the minimization of APL (OF_1) and THD (OF_4) are taken into account at the same time as per (14). THD is a significant factor for NLDG. According to the IEEE 519 Standard, the maximum THD is 5%. The THD level does not exceed the limit for the 33 bus systems above two case studies. The Pareto-optimal front obtained by OARO algorithm is shown in Fig. 4 by varying the weighting factor and optimum point has been also identified using

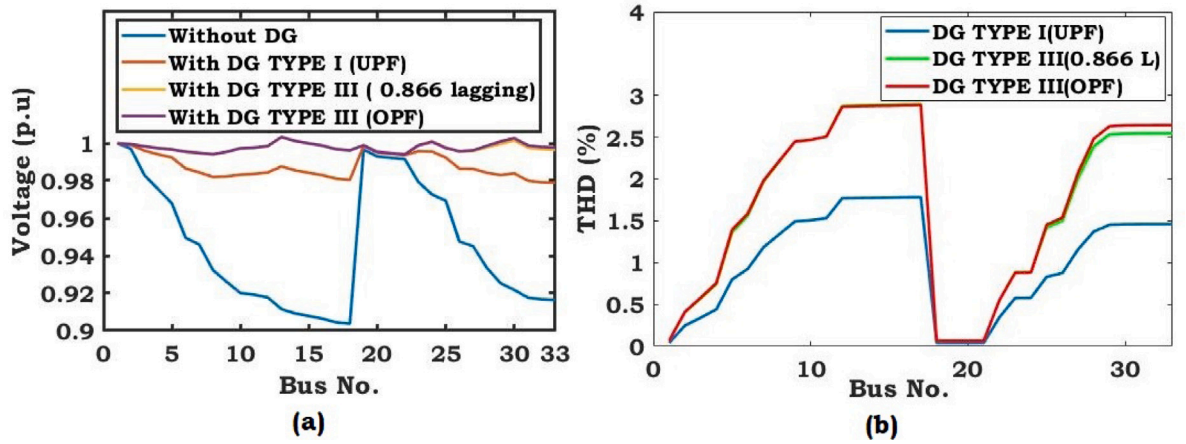

Fig. 2. (a) Voltage profile for case study 2 and (b) THD (%) for case study 3 for IEEE 33 bus.

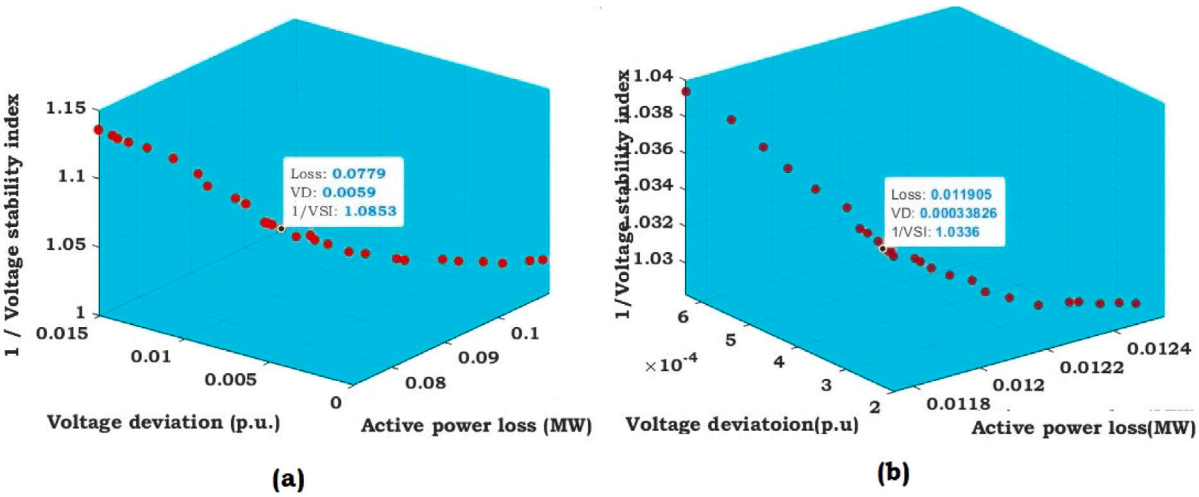

Fig. 3. Pareto-optimal front achieved by OARO algorithm for case study 2 for IEEE 33 bus (a) with DG TYPE I (UPF) and (b) with DG TYPE III (OPF).

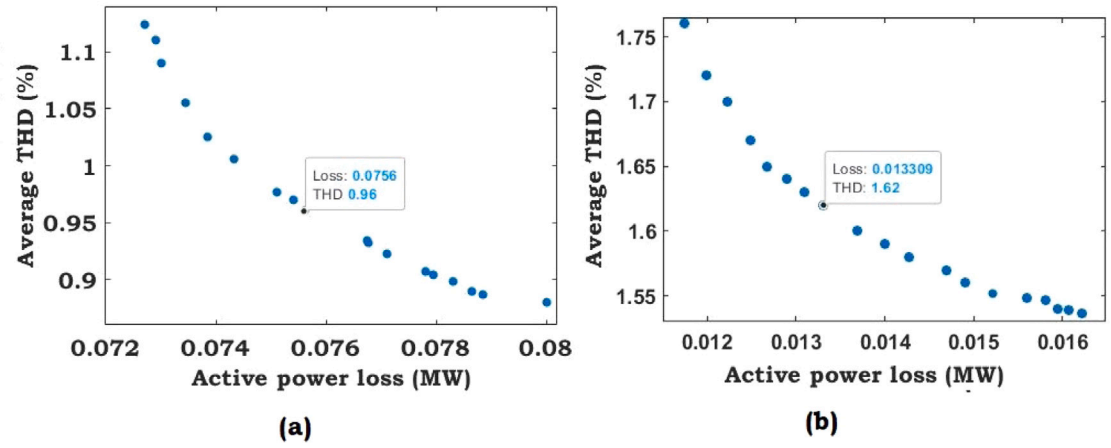

Fig. 4. Pareto-optimal front achieved by OARO algorithm for case study 3 for IEEE 33 bus (a) with DG TYPE I (UPF) and (b) with DG TYPE III (OPF).

Fuzzy based mechanism. Results are shown in Table 5. Network has the lowest THD level for DG TYPE -I. The average THD level is 0.9615% and the maximum THD is 1.75% at bus no. 17. For DG TYPE III at 0.866 lagging power factor, THD is reduced to 2.84%, and for OPF, its value is reduced to 2.8347% at bus no. 17. The THD level is lower in case study 3 compared to case study 1 and case study 2. It is observed that OARO can promptly converge to the best solutions when both OARO and ARO are performed simultaneously. For case 3.1–3.3, power loss is reduced to 75.639 kW, 16.705 kW & 13.309 kW respectively. Fig. 2(b) represents the variation in THD of the 33-bus network with the addition

Table 2
Inverter-based DG harmonics.

Harmonic Oder	Distortion limit (%)	Harmonic Oder	Distortion limit (%)
5	4	29	0.6
7	4	31	0.6
11	2	35	0.3
13	2	37	0.3
17	1.5	41	0.3
19	1.5	43	0.3
23	0.6	47	0.3
25	0.6	49	0.3

of the DG units. The THD at the bus no. 17 is highest at 2.84% for Case 3.2, as seen in the figure, which is noticeably lower than Case Study 1 and Case Study 2. The results of this study show that choosing the optimal power factor value is essential for both loss minimization and THD minimization.

5.2. RDS 3: IEEE 118-bus

5.2.1. Case study 1: Active power loss minimization

On a large-scale RDN with 118 buses, the effectiveness of the suggested strategy is demonstrated. Table 6, 7 and 8 show the best positions and dimensions for DG units determined by OARO and ARO for all scenarios. For Case 1.1–1.3, the real power loss values determined by OARO are 514.883 kW, 145.475 kW, and 125.751 kW, while the values attained by ARO are 515.083 kW, 145.475 kW, and 126.17 kW, respectively. The APL achieved with OARO is 514.883 kW superior to the 518.653 kW obtained from QODELFA [20], the 516.2658 kW from QOCSOS [11], and the 525.277 kW from SFSA [42], based on the comparison shown in Table 6. By adopting the suggested OARO, the APL is further decreased to 145.475 kW for DG TYPE III with 0.866 lagging pf. This figure is less than the 148.931 kW reported by QODELFA [20] and the 155.159 kW reported by SFSA [42]. For case 1.2, comparisons are shown in Table 7. According to Table 8, OARO excelled in other comparative techniques including QOCSOS [11], SFSA [42] and regular ARO for Case 1.3 of this scenario. 125.751 kW is the active power loss accomplished by OARO, which is significantly less than the 126.2304 kW from QOCSOS [11], the 126.227 kW from SFSA [42], and the 126.17 kW from ARO. This implied that the system's APL was significantly reduced when DG operating at OPF. During the network's integration of DG units, minimum voltage values by OARO are 0.9566 p.u. (54), 0.9760 p.u. (62), and 0.9760 p.u. (62). In this case, OARO proved to be more successful for the large-scale system than the comparative methods in regard to the efficacy of the solutions. For Case studies, 1.1–1.3, the THD for the 118-bus test network has been increased from 0 (base case) to 3.4%, 5.36%, and 5.41%, respectively, for NLDG at bus 76. It does, however, go over the permitted THD limit. Further THD reduction was also included in this study.

5.2.2. Case study 2: Simultaneous APL and VD minimization, as well as VSI enhancement

In this study the simultaneous reduction of $APL(OF_1)$, $VD(OF_2)$, and $VSI^{-1}(OF3)$ have been chosen as per (13). Pareto optimum front, as attained by OARO, has been used as an effective strategy in this case. Pareto-optimal front obtained by OARO algorithm is shown in Fig. 5. It can be seen from the result shown in Table 9 that the APL and VD are reduced to 554.2 kW and 0.02957 p.u., respectively, while the VSI is increased to 0.8967 p.u. using OARO in case of DG TYPE I. These results are superior to those from SFSA [42] and QODELFA [20]. Nevertheless, the overall solutions of OARO are better than those of other methods. Table 10 displays the result from Case 2.2 with DGs with 0.866 lagging pf. As can be shown, the suggested algorithm provides a better answer considering the three parameters APL (162.365 kW), VD (0.005207 p.u.), and VSI (0.91194 p.u.) contemporaneously than the solutions from SFSA, [42], respectively, 128.3 kW, 0.00551 p.u., and 0.9099 p.u. are achieved when the power factor is adjusted to optimal value (Case 2.3) as shown in Table 11. The voltage profiles of the 118-bus test network are shown in Fig. 7(a) following the integration of DG units attained by OARO for Case 2.1, Case 2.2, and Case 2.3. For Case 2.1, Case 2.2, and Case 2.3, the minimal voltage levels are 0.9731 p.u., 0.9772 p.u., and 0.9767 p.u., respectively, at bus 62 which is far better than the base value (0.869 p.u.). Fig. 1(b) illustrates the convergence characteristics for case study 2 for DG TYPE I by contrasting OARO & ARO showing that OARO converges significantly more quickly than traditional ARO. The 118-bus test network's THD is increased for Cases 2.1–2.3 from 0 (base case) to 3.933%, 5.516%, and 5.4242%, respectively, for NLDG at bus 76. It can be seen that the OPF operation gives lower harmonics than 0.866 lag. However, it exceeds the allowable THD threshold. In this work, further, THD minimization is also included.

5.2.3. Case study 3: Simultaneous minimization of APL and THD

In these investigations, the reduction of $APL(OF_1)$ and $THD(OF_4)$ is regarded as contemporaneous for 118 RDNs. For the RDNs 33 the THD level remains inside the threshold limit *i.e.* 5% for all the case studies, but it has crossed the limit for the RDS 118 network. Pareto-optimal front achieved by OARO algorithm has been shown in Fig. 6. Here, THD reduction becomes necessary. According to Eq. (14), objective function has been formed. The network has the lowest THD level with DG TYPE-I. bus no. 76 has the highest THD level (3.138%), and the average THD level is 1.058%, from the OARO data as shown in Table 12. The results of OARO are significantly better than those of ARO in every case. At bus number 76, THD for DG TYPE III is decreased to 4.7% at a lagging power factor of 0.866 and 4.82% at OPF. The average and maximum THD levels in case study 3 are lower than those in case studies 1 and 2. The variation of THD level in the 118-bus network caused by the inclusion of the DG units is depicted in Fig. 7(b) for case study 3. Considering THD minimization, power loss is reduced to 521.47 kW, 213.8 kW, and 135.516 kW respectively for cases 3.1–3.2. According to the results, Case 3.3 has the highest THD at bus number 76 (4.82%), which is considerably lower than case studies 1 (5.41%) and case study 2 (5.424%). According to the study's findings, a power factor of 0.866 lag provides the best outcomes for both loss minimization and THD reduction. In comparison to the other case studies 1 and 2, it can be noted that the minimization deviation is also at a minimum of 0.00074. By contrasting OARO and ARO, Fig. 1(c) illustrates the convergence rate for case study 3 for DG TYPE I (UPF), indicating that OARO converges much more quickly than conventional ARO.

6. Conclusions

In this research, a new approach for searching for the ideal position and size of distributed generation (DG) units to install in distribution networks is presented. This scheme aims to achieve optimal DG penetration while meeting all network operational parameters. Using the criteria of APL, VD minimization, and VSI enhancement, the OARO approach is employed to survey three parameters of DG unit (DG capacity, power factor, and position) in the 33, and 118-bus RDNs. The Pareto optimal front technique is used for multi-objective problems and the set of Pareto-level solutions is used to determine the optimal solution. APL minimization is also included in this survey. By using the suggested algorithm, superior results can be achieved over many of the prior methods for the three scenarios under study, especially the large IEEE 118-bus system, in comparisons between the proposed OARO as well as many existing algorithms from the research for the two test systems. For instance, APL has been found as 514.883 kW, 145.475 kW, and 125.751 kW for UPF, 0.866 lagging, and OPF, respectively which is better than QOCSOS, QODELFA, and SFSA. APL is reduced up to 60.33%,

Table 3
Results for APL in the 33-bus RDS.

Techniques	Optimal location	Optimal size MVA	MW	MVAR	pf	TOTAL DG INPUT (MVA)	APL (KW)	VD	VSI	Avg. THD	Minimum bus voltage (p.u.)	Weakest bus	Maximum THD (bus no)
Case 1.1: DG TYPE -I [unity power factor]													
	13	0.8011	0.8018	0	1								
OARO	24	1.088	1.089	0	1	2.9429	72.785	0.01514	0.8804	1.124%	0.9687	33	2.10% (17)
	30	1.0538	1.0537	0	1								
	13	0.801	0.801	0	1								
ARO	24	1.089	1.089	0	1	2.944	72.785	0.01509	0.8806	1.12%	0.9687	33	2.107% (17)
	30	1.054	1.054	0	1								
	13	0.8018	0.8018	0	1								
QODELFA [20]	24	1.0913	1.0913	0	1	2.9467	72.785	0.01509	0.8804	_	_	_	_
	30	1.0536	1.0536	0	1								
	13	0.802	0.802	0	1								
SFSA [42]	24	1.092	1.092	0	1	2.9477	72.785	0.01509	0.8805	_	_	_	_
	30	1.0537	1.0537	0	1								
Case 1.2: DG TYPE III with fixed power factor (0.866 lagging)													
	13	0.8755	0.75818	0.4377	0.866								
OARO	24	1.185	1.0269	0.5929	0.866	3.4621	15.347	0.000652	0.96209	1.741%	0.9922	8	3.14% (17)
	30	1.4016	1.2138	0.7008	0.866								
	13	0.8755	0.75818	0.4377	0.866								
ARO	24	1.185	1.0269	0.5929	0.866	3.4621	15.347	0.000652	0.962086	1.741%	0.9922	8	3.14% (17)
	30	1.4016	1.2138	0.7008	0.866								
	13	0.8756	0.7582	0.4378	0.866								
QODELFA [20]	24	1.186	1.0273	0.593	0.866	3.4634	15.347	0.00065	0.9692	_	_	_	_
	30	1.4018	1.2139	0.7009	0.866								
	13	0.985	0.853	0.4925	0.866								
KHA [46]	24	1.0392	0.9	0.5196	0.866	3.0634	19.578	_	0.9286	_	_	_	_
	30	1.0392	0.8999	0.5196	0.866								
Case 1.3: DG TYPE-III with optimum Power Factor													
	13	0.8774	0.79378378	0.3734	0.9047								
OARO	24	1.1883	1.07113362	0.5169	0.9014	3.5089	11.740	0.000633	0.96212	1.768%	0.9922	8	3.13% (17)
	30	1.4432	1.03073344	1.0113	0.7142								
	13	0.88	0.796136	0.3749	0.9047								
ARO	24	1.1884	1.07122376	0.5153	0.9014	3.511	11.741	0.000633	0.96212	1.768%	0.9921	8	3.13% (17)
	30	1.4426	1.03030492	1.0079	0.7142								
	13	0.8772	0.79387	0.37317	0.905								
QOCSOS [11]	24	1.1884	1.07075	0.51555	0.901	3.5083	11.741	_	_	_	_	_	_
	30	1.4427	1.03009	1.01010	0.714								
	13	0.87680	0.7927	0.3747	0.904								
SFSA [42]	24	1.15527	1.03	0.5232	0.892	3.51233	11.762	0.000619	0.9691	_	_	_	_
	30	1.48027	1.0422	1.0512	0.716								

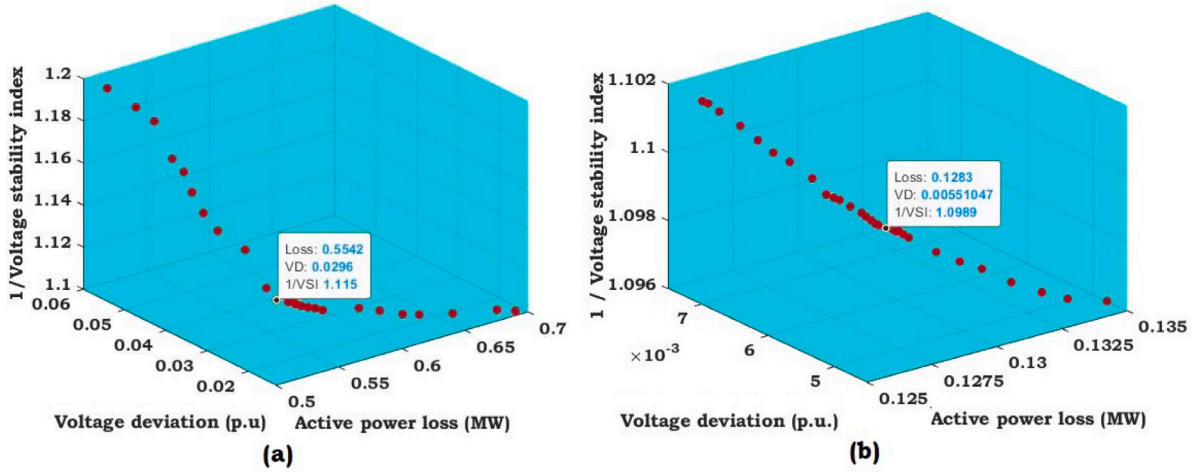

Fig. 5. Pareto-optimal front achieved by OARO algorithm for case study 2 for IEEE 118 bus (a) with DG TYPE I (UPF) and (b) with DG TYPE III (OPF).

88.79%, and 90.32% for UPF, 0.866 lagging, and OPF, respectively. For multi-objective optimization problems, OARO also gives better results like 162.365 kW (APL), 0.005207 (VD), and 0.91194 (VSI) at 0.866 lagging for case study 2 than other algorithms for 118 bus RDN and 15.496 kW (APL), 0.0035 (VD), and 0.9673 (VSI) at 0.866 lagging for case study 2 than other algorithms for 33 bus RDN. It may be concluded

Table 4
Result for simultaneous APL and VD minimization, as well as VSI enhancement for 33 bus RDS.

Techniques	Optimal location	Optimal size				TOTAL DG INPUT (MVA)	APL (KW)	VD	VSI	Avg. THD	Minimum bus voltage (p.u.)	Weakest bus	Maximum THD (bus no)
		MVA	MW	MVAR	pf								
Case 2.1: DG TYPE -I [unity power factor]													
	13	0.9539	0.9539	0	1								
OARO	24	1.1635	1.1635	0	1	3.45	77.873	0.00598	0.9213	1.329%	0.9797	33	2.469% (17)
	30	1.3294	1.3294	0	1								
	13	0.9623	0.9623	0	1								
ARO	24	1.1356	1.1356	0	1	3.400	77.377	0.00626	0.9182	1.323%	0.9789	33	2.47% (17)
	30	1.3026	1.3026	0	1								
	13	0.962292	0.962292	0	1								
MRFO [21]	24	1.1364	1.1364	0	1	3.401192	77.3793	0.0063	0.9182	_	_	_	_
	30	1.3025	1.3025	0	1								
	13	0.9647	0.9647	0	1								
QODELFA [20]	24	1.1334	1.1334	0	1	3.3998	77.408	0.00621	0.9182	_	_	_	_
	30	1.3017	1.3017	0	1								
Case 2.2: DG TYPE-III with fixed power factor (0.866 lagging)													
	13	0.9112	0.7891	0.4556	0.866								
OARO	24	1.1973	1.0369	0.5987	0.866	3.550	15.496	0.0035	0.9673	1.788%	0.994	8	3.23% (17)
	30	1.4392	1.2463	0.7197	0.866								
	13	0.914	0.7915	0.457	0.866								
ARO	24	1.211	1.04873	0.6055	0.866	3.5561	15.493	0.00356	0.967	1.78%	0.994	8	3.23% (17)
	30	1.4311	1.23933	0.71555	0.866								
	13	0.91544	0.79271	0.45772	0.866								
MRFO [21]	24	1.2007	1.0397	0.60035	0.866	3.54764	15.4956	0.00354	0.967	_	_	_	_
	30	1.4315	1.2396	0.71575	0.866								
	13	0.9134	0.7911	0.4567	0.866								
QODELFA [20]	24	1.1982	1.0411	0.5991	0.866	3.5472	15.498	0.0035	0.9671	_	_	_	_
	30	1.4356	1.2431	0.7178	0.866								
Case 2.3: DG TYPE-III with optimum power factor													
	13	0.9101	0.8218	0.3910	0.903								
OARO	24	1.2041	1.0765	0.5595	0.894	3.58	11.905	0.000338	0.96751	1.815%	0.994	8	3.227% (17)
	30	1.485	1.0677	1.0325	0.719								
	13	0.917959	0.8308	0.3905	0.905								
ARO	24	1.1877	1.0618	0.5322	0.894	3.58	11.897	0.000334	0.9672	1.815%	0.994	8	3.287% (17)
	30	1.4755	1.0609	1.0255	0.719								
	13	0.9083	0.809912	0.41127	0.8916								
MRFO [21]	24	1.2038	1.079	0.5339	0.8963	3.5896	11.918	0.000338	0.9674	_	_	_	_
	30	1.4775	1.0724	1.0162	0.7258								
	13	0.92154	0.834	0.3916	0.905								
SFSA [42]	24	1.1897	1.0648	0.5314	0.895	3.58644	11.911	0.000334	0.9675	_	_	_	_
	30	1.4752	1.0592	1.0259	0.718								

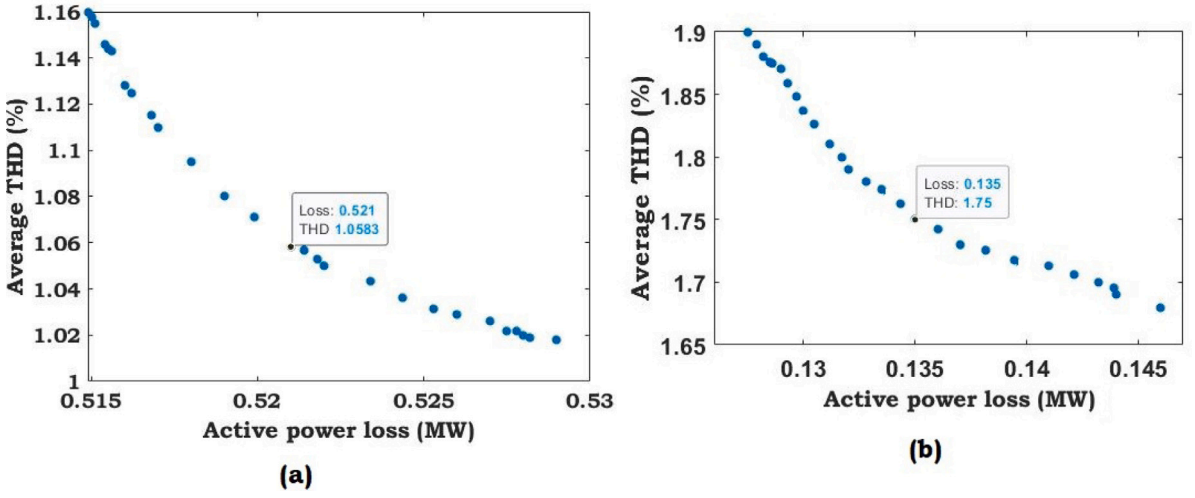

Fig. 6. Pareto-optimal front achieved by OARO algorithm for case study 3 for IEEE 118 bus (a) with DG TYPE I (UPF) and (b) with DG TYPE III (OPF).

that OARO is a very appealing optimization technique for resolving complex and large distribution networks for optimal DG placement and sizing issues. The harmonic analysis is ignored in most of the recent studies. For the large network like 118 bus, it has been seen that the

Table 5
Simultaneous minimization of APL and THD.

Techniques	Optimal location	Optimal size				TOTAL DG INPUT (MVA)	APL (KW)	VD	VSI	Avg. THD	Minimum bus voltage (p.u.)	Weakest bus	Maximum THD (bus no)
		MVA	MW	MVAR	pf								
Case 3.1: DG TYPE -I [unity power factor]													
	13	0.6216	0.6216	0	1								
OARO	24	1.055	1.055	0	1	2.62	75.639	0.0253	0.8476	0.9615%	0.9576	18	1.75% (17)
	30	0.943	0.943	0	1								
	13	0.7289	0.7289	0	1								
ARO	24	0.9375	0.9375	0	1	2.60	74.35	0.0215	0.8587	1.017%	0.9627	18	1.92% (17)
	30	0.9293	0.9293	0	1								
Case 3.2: DG TYPE-III with fixed power factor (0.866 lagging)													
	13	0.7614	0.6594	0.3807	0.866								
OARO	24	1.091	0.9448	0.5455	0.866	3.17	16.705	0.002794	0.9391	1.59%	0.9844	18	2.84% (17)
	30	1.321	1.144	0.6606	0.866								
	14	0.695	0.60187	0.3475	0.866								
ARO	24	1.283	1.111	0.6415	0.866	3.306	17.086	0.003067	0.9405	1.597%	0.9848	18	2.9071% (17)
	30	1.328	1.15	0.664	0.866								
Case 3.2: DG TYPE-III with optimum power factor													
	13	0.806738	0.7688	0.244	0.953								
OARO	24	1.241	1.0921	0.5894	0.88	3.38	13.309	0.00243	0.9422	1.62%	0.9852	18	2.8347% (17)
	30	1.33	0.9480	0.9328	0.7128								
	13	0.8038	0.7628	0.2534	0.949								
ARO	24	1.253	1.1089	0.5834	0.885	3.38	13.274	0.00251	0.9418	1.625%	0.9852	18	2.84% (17)
	30	1.321	0.9287	0.9395	0.703								

Table 6
Results for APL in the 118-bus RDS.

Techniques	Optimal location	Optimal size				TOTAL DG INPUT (MVA)	APL (KW)	VD	VSI	Avg. THD	Minimum bus voltage (p.u.)	Weakest bus	Maximum THD (bus no)
		MVA	MW	MVAR	pf								
Case 1.1: DG TYPE -I [unity power factor]													
	30	3.671	3.671	0	1								
	42	1.15	1.15	0	1								
	50	2.3326	2.3326	0	1								
OARO	72	2.529	2.529	0	1	16.5566	514.883	0.05868	0.83743	1.16%	0.9566	54	3.4% (76)
	80	2.091	2.091	0	1								
	96	1.658	1.658	0	1								
	109	3.125	3.125	0	1								
	20	1.79	1.79	0	1								
	41	1.83	1.83	0	1								
	50	2.7316	2.7316	0	1								
ARO	72	2.533	2.533	0	1	15.7352	515.038	0.0577	0.8364	1.16%	0.9563	54	3.41% (76)
	80	2.09	2.09	0	1								
	96	1.6716	1.6716	0	1								
	109	3.089	3.089	0	1								
	30	3.7083	3.7083	0	1								
	42	1.1543	1.1543	0	1								
	50	2.3338	2.3338	0	1								
QOCSOS [11]	73	2.417	2.417	0	1	16.5282	516.2658	_	_	_	0.9546	_	_
	80	2.1072	2.1072	0	1								
	96	1.6877	1.6877	0	1								
	109	3.1199	3.1199	0	1								
	20	1.7908	1.7908	0	1								
	39	2.7341	2.7341	0	1								
	47	1.8329	1.8329	0	1								
QODELFA [20]	73	2.4034	2.4034	0	1	15.606	518.653	0.0578	0.8245	_	_	_	_
	80	1.7505	1.7505	0	1								
	90	2.2945	2.2945	0	1								
	110	2.7998	2.7998	0	1								
	21	1.3757	1.3757	0	1								
	42	1.1997	1.1997	0	1								
	50	2.7418	2.7418	0	1								
SFSA [42]	71	2.8915	2.8915	0	1	13.9115	525.277	0.0612	0.8271	_	_	_	_
	81	1.7025	1.7025	0	1								
	97	1.3329	1.3329	0	1								
	110	2.6674	2.6774	0	1								

THD level is increased above 5%, for example, 5.36%, and 5.41% at bus 76 for 0.866 lagging and OPF, respectively for case study 1 and 5.516%, and 5.4242% at bus 76 for 0.866 lagging and OPF respectively for case study 2, which is very significant for nonlinear type DG (NLDG)

Table 7
Results for APL in the 118-bus RDS.

Techniques	Optimal location	Optimal size				TOTAL DG INPUT (MVA)	APL (KW)	VD	VSI	Avg. THD	Minimum bus voltage (p.u.)	Weakest bus	Maximum THD (bus no)
		MVA	MW	MVAR	pf								
Case 1.2: DG TYPE-III with fixed power factor (0.866 lagging)													
	20	2.1238	1.8392	1.0619	0.866								
	41	2.2185	1.9212	1.1093	0.866								
	50	3.687	3.1929	1.8435	0.866	19.0763	145.475	0.007817	0.9072	1.866%	0.976	62	5.36% (76)
OARO	76	2.773	2.4014	1.3865	0.866								
	80	2.64	2.2862	1.3200	0.866								
	96	1.987	1.7207	0.9935	0.866								
	110	3.647	3.1583	1.8235	0.866								
	20	2.1238	1.8392	1.0619	0.866								
	41	2.2185	1.9212	1.1093	0.866								
	50	3.687	3.1929	1.8435	0.866								
ARO	76	2.773	2.4014	1.3865	0.866	19.0763	145.475	0.007817	0.9072	1.86%	0.976	62	5.36% (76)
	80	2.64	2.2862	1.3200	0.866								
	96	1.987	1.7207	0.9935	0.866								
	110	3.647	3.1583	1.8235	0.866								
	21	2.2345	1.9351	1.1174	0.866								
	40	2.4030	2.081	1.2016	0.866								
	50	3.6144	3.1301	1.8074	0.866								
SFSA [42]	71	3.3395	2.892	1.6699	0.866	19.2943	155.159	0.008607	0.9078	_	_	_	_
	80	2.3720	2.0541	1.1861	0.866								
	96	1.6004	1.3859	0.8003	0.866								
	110	3.7305	3.2306	1.8654	0.866								
	20	2.1676	1.8771	1.0838	0.866								
	39	3.5692	3.0909	1.7846	0.866								
	46	2.5144	2.1775	1.2572	0.866								
QODELFA [20]	74	2.7241	2.3591	1.3621	0.866	19.3658	148.931	0.0086	0.9071	_	_	_	_
	85	1.9657	1.7023	0.9829	0.866								
	90	2.8309	2.4516	1.4156	0.866								
	110	3.5939	3.1123	1.7971	0.866								

Table 8
Results for APL in the 118-bus RDS.

Techniques	Optimal location	Optimal size				TOTAL DG INPUT (MVA)	APL (KW)	VD	VSI	Avg. THD	Minimum bus voltage (p.u.)	Weakest bus	Maximum THD (bus no)
		MVA	MW	MVAR	pf								
Case 1.3: DG TYPE-III with optimum power factor													
	20	2.1230	1.7472	1.206	0.823								
	41	2.218	1.8920	1.1575	0.853								
	50	3.687	2.8058	2.3919	0.761								
OARO	74	2.773	2.3571	1.4608	0.85	19.0750	125.751	0.007269	0.9074	1.90%	0.976	62	5.41% (76)
	80	2.64	2.0568	1.6550	0.7791								
	96	1.9870	1.6572	1.0964	0.834								
	110	3.6470	2.7972	2.3401	0.767								
	20	2.1755	1.8337	1.1706	0.8429								
	41	2.2253	1.8790	1.1921	0.8444								
	50	3.6586	2.7440	2.4199	0.75								
ARO	74	2.7356	2.3389	1.4187	0.855	19.0265	126.17	0.00749	0.9074	1.89%	0.976	62	5.41% (76)
	80	2.616	1.9620	1.73	0.75								
	96	1.9863	1.7051	1.0189	0.8584								
	110	3.6292	2.7219	2.4	0.75								
	20	2.1954	1.7871	1.2752	0.814								
	41	2.2178	1.8164	1.2726	0.819								
	50	3.668	2.7070	2.4752	0.738								
QOCSOS [11]	74	2.7369	2.2963	1.4892	0.839	19.0586	126.2304	_	_	_	_	_	_
	80	2.6128	2.0850	1.5746	0.798								
	96	1.9876	1.6696	1.0784	0.84								
	110	3.6401	2.7992	2.3269	0.769								
	20	2.18961	1.7861	1.2666	0.816								
	41	2.2188	1.82	1.2692	0.82								
	50	3.66924	2.7122	2.4713	0.739								
SFSA [42]	74	2.73298	2.2975	1.4801	0.841	19.04543224	126.227	0.007413	0.9075	_	_	_	_
	80	2.61568	2.08555	1.5787	0.797								
	96	1.9849	1.6697	1.0734	0.841								
	110	3.63409	2.7995	2.3172	0.77								

installation. The system includes additional optimal sizing and power factor searching, taking into account the minimization of the average THD of the whole system and the maximum THD of a specific bus. Therefore, OARO implementation for better-optimizing results of large-scale OPDG Problems and harmonic analysis is the core factor of this work considering different types of DG.

Table 9
Result for simultaneous APL and VD minimization, as well as VSI enhancement in 118-bus RDS.

Techniques	Optimal location	Optimal size				TOTAL DG INPUT (MVA)	APL (KW)	VD	VSI	Avg. THD	Minimum bus voltage (p.u.)	Weakest bus	Maximum THD (bus no)
		MVA	MW	MVAR	pf								
Case 2.1: DG TYPE -I [unity power factor]													
	20	2.114	2.114	0	1								
	41	2.143	2.143	0	1								
	50	3.8943	3.8943	0	1								
OARO	73	2.861	2.861	0	1	18.90	554.2	0.02957	0.8967	1.396%	0.9731	54	3.96% (76)
	80	2.478	2.478	0	1								
	91	2.121	2.121	0	1								
	110	3.291	3.291	0	1								
	20	2.132	2.132	0	1								
	41	2.169	2.169	0	1								
	50	3.865	3.865	0	1								
ARO	73	2.852	2.852	0	1	18.91	553.516	0.0294	0.8953	1.66%	0.9727	54	3.933% (76)
	80	2.483	2.483	0	1								
	96	1.996	1.996	0	1								
	110	3.4100	3.41	0	1								
	20	2.1256	2.1256	0	1								
	39	3.8797	3.8797	0	1								
	47	2.3173	2.3173	0	1								
QODELFA [20]	73	2.8518	2.8518	0	1	18.9289	554.682	0.0297	0.8889	–	–	–	–
	80	2.0957	2.0957	0	1								
	91	2.4212	2.4212	0	1								
	110	3.2376	3.2376	0	1								
	19	2.0313	2.0313	0	1								
	41	1.9135	1.9135	0	1								
	49	4.0113	4.0113	0	1								
SFSA [42]	73	2.7996	2.7996	0	1	19.7346	564.104	0.030852	0.8757	–	–	–	–
	79	3.0734	3.0734	0	1								
	96	2.0861	2.0861	0	1								
	108	3.8194	3.8194	0	1								

Table 10
Result for simultaneous APL and VD minimization, as well as VSI enhancement in 118-bus RDS.

Techniques	Optimal location	Optimal size				TOTAL DG INPUT (MVA)	APL (KW)	VD	VSI	Avg. THD	Minimum bus voltage (p.u.)	Weakest bus	Maximum THD (bus no)
		MVA	MW	MVAR	pf								
Case 2.2: DG TYPE-III with fixed power factor (0.866 lagging)													
	20	2.351	2.0360	1.17560	0.866								
	41	2.6916	2.3309	1.3459	0.866								
	50	4.2592	3.6885	2.1298	0.866								
OARO	74	2.8213	2.4432	1.4108	0.866	21.42	162.365	0.005207	0.91194	2.0%	0.9772	62	5.516% (76)
	80	2.8597	2.4765	1.43	0.866								
	91	2.518	2.1806	1.2591	0.866								
	110	3.9415	3.405	1.9577	0.866								
	20	2.349	2.0342	1.0746	0.866								
	41	2.6895	2.3291	1.3449	0.866								
	50	4.2713	3.6989	2.1358	0.866								
ARO	72	2.792	2.4179	1.3961	0.866	21.39	167.13	0.00566311	0.91197	2.025%	0.977	62	5.34% (76)
	80	2.8457	2.4644	1.4230	0.866								
	91	2.523	2.1849	1.2616	0.866								
	110	3.917	3.3921	1.9586	0.866								
	19	2.1309	1.8454	1.0655	0.866								
	39	2.5473	2.206	1.2737	0.866								
	50	4.2218	3.6561	2.1109	0.866								
SFSA [42]	74	2.6141	2.2638	1.3070	0.866	20.7032	176.969	0.008519	0.9109	–	–	–	–
	80	2.8238	2.4454	1.4119	0.866								
	90	2.3505	2.0355	1.1752	0.866								
	108	4.0148	3.4768	2.0074	0.866								

7. Future scopes

This analysis looks for the best locations for DGs throughout the network of 33, and 118 bus RDNs, depending on the type. These DG units might meet the technical requirements for the least amount of power loss, voltage deviation, voltage stability index, and THD, but they might not satisfy the requirements for the economic component (*i.e.*, investment cost, and operating cost).

Three DG are installed for the RDN 33 network, and seven DG are installed for the RDN 118 network. It is achievable to raise the number of DG throughout the system by choosing more than one objective. The OPDG problem may be described as an integrated multi-objective combination of different economic and technological issues to evaluate the ideal number of DG units in the future.

Improved searching skills may enable the proposed algorithm to be advanced, enhancing its exploitation and exploration potential.

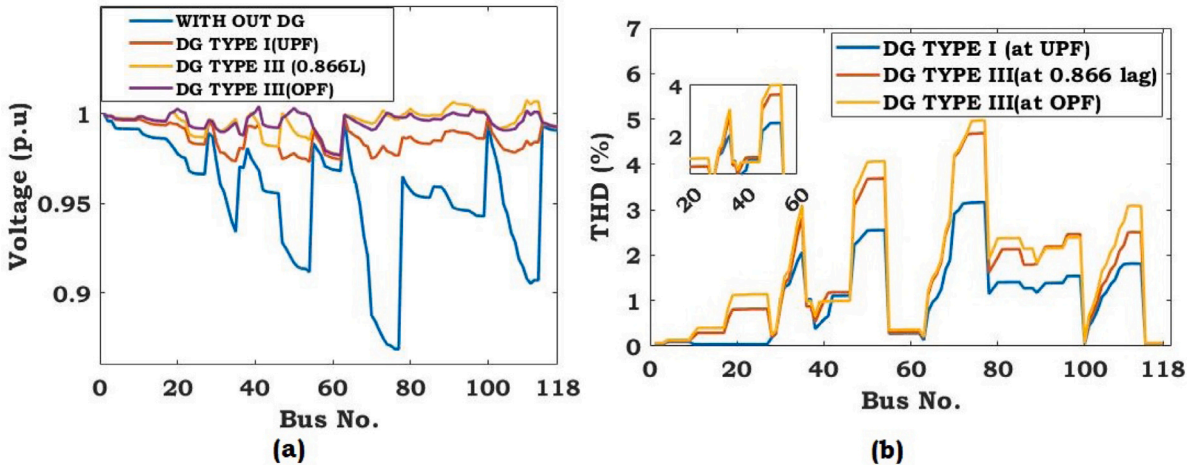

Fig. 7. (a) Voltage profile for case study 2 and (b) THD (%) for case study 3 for IEEE 118 bus.

Table 11
Result for simultaneous APL and VD minimization, as well as VSI enhancement in the 118-bus RDS.

Techniques	Optimal location	Optimal size				TOTAL DG INPUT (MVA)	APL (KW)	VD	VSI	Avg. THD	Minimum bus voltage (p.u.)	Weakest bus	Maximum THD (bus no)
		MVA	MW	MVAR	pf								
Case 2.3: DG TYPE-III with optimum power factor													
	20	2.341	1.9032	1.3631	0.818								
	41	2.5952	2.0691	1.4450	0.818								
	50	3.8815	2.8375	2.6486	0.731								
OARO	74	2.7556	2.3423	1.4516	0.85	20.15	128.3	0.005510	0.9099	1.98%	0.9767	62	5.4242% (76)
	80	2.6715	2.1132	1.6345	0.791								
	96	2.156	1.7981	1.1896	0.834								
	110	3.818	2.9475	2.4268	0.772								
	20	2.341	1.9032	1.3631	0.818								
	41	2.5952	2.0691	1.4450	0.818								
	50	3.8815	2.8375	2.6486	0.731								
OARO	74	2.7556	2.3423	1.4516	0.85	20.15	128.3	0.005510	0.9099	1.98%	0.9767	62	5.4242% (76)
	80	2.6715	2.1132	1.6345	0.791								
	96	2.156	1.7981	1.1896	0.834								
	110	3.818	2.9475	2.4268	0.772								
	20	2.3243	1.8548	1.4025	0.798								
	41	2.4771	2.0279	1.4225	0.818								
	50	3.8575	2.8391	2.6147	0.736								
SFSA [42]	74	2.8078	2.3698	1.5045	0.844	19.8706	128.105	0.005796	0.9095	–	–	–	5.47% (76)
	80	2.6697	2.1251	1.6172	0.796								
	96	2.0071	1.6639	1.1245	0.829								
	110	3.7271	2.8736	2.3758	0.771								

Table 12
Result for simultaneous APL and THD minimization in the 118-bus RDS.

Techniques	Optimal location	Optimal size				TOTAL DG INPUT (MVA)	APL (KW)	VD	VSI	Avg. THD	Minimum bus voltage (p.u.)	Weakest bus	Maximum THD (bus no)
		MVA	MW	MVAR	pf								
Case 3.1: DG TYPE -I [unity power factor]													
	30	3.4709	3.4709	0	1								
	42	0.989	0.989	0	1								
	50	1.951	1.951	0	1								
OARO	72	2.293	2.293	0	1	15.12	521.47	0.07319	0.8160	1.058%	0.9505	54	3.138% (76)
	80	1.805	1.805	0	1								
	96	1.603	1.603	0	1								
	109	3.012	3.012	0	1								
	20	2.15	2.15	0	1								
	41	1.4760	1.4760	0	1								
	50	2.4853	2.4853	0	1								
ARO	72	2.4376	2.319	0	1	13.87	547.76	0.0797	0.8198	1.045%	0.9516	54	3.27% (76)
	80	1.9132	1.9132	0	1								
	90	1.498	1.498	0	1								
	110	1.91	1.91	0	1								

(*continued on next page*)

Table 12 (*continued*).

Techniques	Optimal location	Optimal size MVA	MW	MVAR	pf	TOTAL DG INPUT (MVA)	APL (KW)	VD	VSI	Avg. THD	Minimum bus voltage (p.u.)	Weakest bus	Maximum THD (bus no)
Case 3.2: DG TYPE-III with fixed power factor (0.866 lagging)													
	19	1.493	1.2929	0.7466	0.866								
	39	1.46	1.2644	0.7301	0.866								
	50	2.998	2.5963	1.499	0.866								
OARO	74	2.4956	2.16	1.2479	0.866	14.86	213.8	0.0308	0.8727	1.50%	0.9665	54	4.7% (76)
	81	1.9560	1.6939	0.9781	0.866								
	96	2.050	1.7753	1.0251	0.866								
	110	2.3170	2.0065	1.1586	0.866								
	19	1.4230	1.2323	0.7115	0.866								
	40	1.7290	1.4973	0.8645	0.866								
	50	2.7890	2.4153	1.3945	0.866								
ARO	73	2.4820	2.1494	1.2410	0.866	15.0840	191.82	0.0272	0.8973	1.51%	0.9733	54	4.64% (76)
	81	1.6980	1.4705	0.8490	0.866								
	96	2.1280	1.8428	1.0640	0.866								
	110	2.8350	2.4551	1.4175	0.866								
Case 3.3: DG TYPE-III with optimum power factor													
	20	1.915	1.5760	1.0878	0.823								
	41	1.858	1.5143	1.0766	0.815								
	50	3.097	2.2949	2.0797	0.741								
OARO	73	2.49	2.1140	1.3157	0.849	17.63	135.516	0.01382	0.90430	1.75%	0.9748	62	4.82% (76)
	80	2.64	2.0618	1.6488	0.781								
	96	1.987	1.6591	1.0933	0.835								
	110	3.647	2.7608	2.3830	0.757								
	20	2.050	1.6585	1.2050	0.809								
	40	2.38	2.094	1.2185	0.859								
	50	2.887	2.1826	1.889	0.756								
ARO	73	2.515	2.1423	1.3175	0.8518	17.56	140.982	0.01605	0.9044	1.72%	0.9752	62	4.79% (76)
	80	2.495	1.8737	1.6475	0.751								
	96	1.815	1.4974	1.0257	0.825								
	110	3.417	2.5662	2.2563	0.751								

CRediT authorship contribution statement

Anamika Ghorai: Conceptualization and Methodology, Algorithm development, Simulation, literature review, Visualization, Investigation. **Barun Mandal:** Editing and Supervision. **Provas Kumar Roy:** Writing, review & editing, Supervision. **Chandan Paul:** Algorithm development, Simulation, Literature Survey, Writing, Reviewing and Editing, Supervision.

Declaration of competing interest

The authors declare the following financial interests/personal relationships which may be considered as potential competing interests: Anamika Ghorai reports was provided by Adyapeath Annada Polytechnic College, Dakhineswar, West Bengal, India.

Data availability

Data will be made available on request.

References

[1] Thomas Ackermann, Göran Andersson, Lennart Söder, Distributed generation: A definition, Electr. Power Syst. Res. 57 (3) (2001) 195–204.

[2] Prasenjit Basak, S. Chowdhury, S. Halder nee Dey, S.P. Chowdhury, A literature review on integration of distributed energy resources in the perspective of control, protection and stability of microgrid, Renew. Sustain. Energy Rev. 16 (8) (2012) 5545–5556.

[3] H.R. Baghaee, M. Mirsalim, M.J. Sanjari, G.B. Gharehpetian, Effect of type and interconnection of DG units in the fault current level of distribution networks, in: 2008 13th International Power Electronics and Motion Control Conference, IEEE, 2008, pp. 313–319.

[4] W. Ei-Khattam, M.M.A. Salama, Distributed generation technologies, definitions and benefits, Electr. Power Syst. Res. 71 (2004) 119–128.

[5] Y.M. Atwa, E.F. El-Saadany, M.M.A. Salama, R. Seethapathy, Optimal renewable resources mix for distribution system energy loss minimization, IEEE Trans. Power Syst. 25 (1) (2009) 360–370.

[6] Vichakorn Hengsritawat, Thavatchai Tayjasanant, Natthaphob Nimpitiwan, Optimal sizing of photovoltaic distributed generators in a distribution system with consideration of solar radiation and harmonic distortion, Int. J. Electr. Power Energy Syst. 39 (1) (2012) 36–47.

[7] Institute of Electrical, Electronics Engineers, IEEE Recommended Practice and Requirements for Harmonic Control in Electric Power Systems, IEEE, 2014.

[8] Bo Yang, Lei Yu, Yixuan Chen, Haoyin Ye, Ruining Shao, Hongchun Shu, Tao Yu, Xiaoshun Zhang, Liming Sun, Modelling, applications, and evaluations of optimal sizing and placement of distributed generations: A critical state-of-the-art survey, Int. J. Energy Res. 45 (3) (2021) 3615–3642.

[9] Ali Ahmed, Muhammad Faisal Nadeem, Arooj Tariq Kiani, Irfan Khan, An overview on optimal planning of distributed generation in distribution system and key issues, in: 2021 IEEE Texas Power and Energy Conference, TPEC, 2021, pp. 1–6, http://dx.doi.org/10.1109/TPEC51183.2021.9384976.

[10] Hussein Abdel-Mawgoud, Salah Kamel, Adel A Abou El-Ela, Francisco Jurado, Optimal allocation of DG and capacitor in distribution networks using a novel hybrid MFO-SCA method, Electr. Power Compon. Syst. 49 (3) (2021) 259–275.

[11] Khoa Hoang Truong, Perumal Nallagownden, Irraivan Elamvazuthi, Dieu Ngoc Vo, An improved meta-heuristic method to maximize the penetration of distributed generation in radial distribution networks, Neural Comput. Appl. 32 (14) (2020) 10159–10181.

[12] Sneha Sultana, Provas Kumar Roy, Multi-objective quasi-oppositional teaching learning based optimization for optimal location of distributed generator in radial distribution systems, Int. J. Electr. Power Energy Syst. 63 (2014) 534–545.

[13] Mohammad Hasan Moradi, M. Abedini, A combination of genetic algorithm and particle swarm optimization for optimal DG location and sizing in distribution systems, Int. J. Electr. Power Energy Syst. 34 (1) (2012) 66–74.

[14] Sharmistha Sharma, Subhadeep Bhattacharjee, Aniruddha Bhattacharya, Quasi-oppositional swine influenza model based optimization with quarantine for optimal allocation of DG in radial distribution network, Int. J. Electr. Power Energy Syst. 74 (2016) 348–373.

[15] Satish Kansal, Vishal Kumar, Barjeev Tyagi, Optimal placement of different type of DG sources in distribution networks, Int. J. Electr. Power Energy Syst. 53 (2013) 752–760.

[16] Imran Ahmad Quadri, S. Bhowmick, D. Joshi, A comprehensive technique for optimal allocation of distributed energy resources in radial distribution systems, Appl. Energy 211 (2018) 1245–1260.

[17] D. Nageswari, N. Kalaiarasi, G. Geethamahalakshmi, Optimal placement and sizing of distributed generation using metaheuristic algorithm, Comput. Syst. Sci. Eng. 41 (2) (2022) 493–509.

[18] Mohamed A. Elseify, Salah Kamel, Hussein Abdel-Mawgoud, Ehab E. Elattar, A novel approach based on honey badger algorithm for optimal allocation of multiple DG and capacitor in radial distribution networks considering power loss sensitivity, Mathematics 10 (12) (2022) 2081.
[19] U. Sultana, Azhar B. Khairuddin, A.S. Mokhtar, N. Zareen, Beenish Sultana, Grey wolf optimizer based placement and sizing of multiple distributed generation in the distribution system, Energy 111 (2016) 525–536.
[20] Rabea Jamil Mahfoud, Yonghui Sun, Nizar Faisal Alkayem, Hassan Haes Alhelou, Pierluigi Siano, Miadreza Shafie-khah, A novel combined evolutionary algorithm for optimal planning of distributed generators in radial distribution systems, Appl. Sci. 9 (16) (2019) 3394.
[21] Mahmoud G. Hemeida, Salem Alkhalaf, Al-Attar A. Mohamed, Abdalla Ahmed Ibrahim, Tomonobu Senjyu, Distributed generators optimization based on multi-objective functions using manta rays foraging optimization algorithm (MRFO), Energies 13 (15) (2020) 3847.
[22] E.S. Ali, S.M. Abd Elazim, A.Y. Abdelaziz, Ant lion optimization algorithm for renewable distributed generations, Energy 116 (2016) 445–458.
[23] Subhodip Saha, Vivekananda Mukherjee, Optimal placement and sizing of DGs in RDS using chaos embedded SOS algorithm, IET Gener. Transm. Distrib. 10 (14) (2016) 3671–3680.
[24] Sajjan Kumar, Kamal K. Mandal, Niladri Chakraborty, Optimal DG placement by multi-objective opposition based chaotic differential evolution for techno-economic analysis, Appl. Soft Comput. 78 (2019) 70–83.
[25] S.A. Syed Mustaffa, I. Musirin, M.K. Mohamad Zamani, M.M. Othman, Pareto optimal approach in multi-objective chaotic mutation immune evolutionary programming (MOCMIEP) for optimal distributed generation photovoltaic (DGPV) integration in power system, Ain Shams Eng. J. 10 (4) (2019) 745–754.
[26] Ahmed S. Abbas, Ragab A. El-Sehiemy, Adel Abou El-Ela, Eman Salah Ali, Karar Mahmoud, Matti Lehtonen, Mohamed M.F. Darwish, Optimal harmonic mitigation in distribution systems with inverter based distributed generation, Appl. Sci. 11 (2) (2021) 774.
[27] Thang Trung Nguyen, Thai Dinh Pham, Le Chi Kien, Le Van Dai, Improved coyote optimization algorithm for optimally installing solar photovoltaic distribution generation units in radial distribution power systems, Complexity 2020 (2020).
[28] Shradha Singh Parihar, Nitin Malik, Analysing the impact of optimally allocated solar PV-based DG in harmonics polluted distribution network, Sustain. Energy Technol. Assess. 49 (2022) 101784.
[29] Ahmad Eid, Salah Kamel, Mohamed H. Hassan, Baseem Khan, A comparison study of multi-objective bonobo optimizers for optimal integration of distributed generation in distribution systems, Front. Energy Res. 10 (2022) 847495.
[30] Ahmad Eid, Hassan El-Kishky, Multi-objective archimedes optimization algorithm for optimal allocation of renewable energy sources in distribution networks, in: International Conference on Digital Technologies and Applications, Springer, 2021, pp. 65–75.
[31] Mohamed Hashem, Mazen Abdel-Salam, Mohamed Th El-Mohandes, Mohamed Nayel, Mohamed Ebeed, Optimal placement and sizing of wind turbine generators and superconducting magnetic energy storages in a distribution system, J. Energy Storage 38 (2021) 102497.
[32] Mohamed Hashem, Mazen Abdel-Salam, Mohamed Nayel, Mohamed Th El-Mohandes, A bi-level optimizer for reliability and security assessment of a radial distribution system supported by wind turbine generators and superconducting magnetic energy storages, J. Energy Storage 51 (2022) 104356.
[33] Rajagopal Peesapati, Vinod Kumar Yadav, Niranjan Kumar, Flower pollination algorithm based multi-objective congestion management considering optimal capacities of distributed generations, Energy 147 (2018) 980–994.
[34] Minh Quan Duong, Thai Dinh Pham, Thang Trung Nguyen, Anh Tuan Doan, Hai Van Tran, Determination of optimal location and sizing of solar photovoltaic distribution generation units in radial distribution systems, Energies 12 (1) (2019) 174.
[35] Liying Wang, Qingjiao Cao, Zhenxing Zhang, Seyedali Mirjalili, Weiguo Zhao, Artificial rabbits optimization: A new bio-inspired meta-heuristic algorithm for solving engineering optimization problems, Eng. Appl. Artif. Intell. 114 (2022) 105082.
[36] Bindeshwar Singh, V. Mukherjee, Prabhakar Tiwari, A survey on impact assessment of DG and FACTS controllers in power systems, Renew. Sustain. Energy Rev. 42 (2015) 846–882.
[37] J.-H. Teng, S.-H. Liao, R.-C. Leou, Three-phase harmonic analysis method for unbalanced distribution systems, Energies 7 (1) (2014) 365–384.
[38] Selcuk Sakar, Murat E. Balci, Shady H.E. Abdel Aleem, Ahmed F. Zobaa, Increasing PV hosting capacity in distorted distribution systems using passive harmonic filtering, Electr. Power Syst. Res. 148 (2017) 74–86.
[39] Dispersed Generation Photovoltaics, Energy Storage, IEEE application guide for IEEE Std 1547™, IEEE standard for interconnecting distributed resources with electric power systems, 2009, IEEE std, 1547–2.
[40] Ahmad Eid, Salah Kamel, Hossam M. Zawbaa, Mostafa Dardeer, Improvement of active distribution systems with high penetration capacities of shunt reactive compensators and distributed generators using Bald Eagle Search, Ain Shams Eng. J. 13 (6) (2022) 101792.
[41] Ahmad Eid, Salah Kamel, Essam H. Houssein, An enhanced equilibrium optimizer for strategic planning of PV-BES units in radial distribution systems considering time-varying demand, Neural Comput. Appl. 34 (19) (2022) 17145–17173.
[42] Tri Phuoc Nguyen, Dieu Ngoc Vo, A novel stochastic fractal search algorithm for optimal allocation of distributed generators in radial distribution systems, Appl. Soft Comput. 70 (2018) 773–796.
[43] Thomas M. Blooming, Daniel J. Carnovale, Application of IEEE Std 519-1992 harmonic limits, in: Conference Record of 2006 Annual Pulp and Paper Industry Technical Conference, IEEE, 2006, pp. 1–9.
[44] Mazen Abdel-Salam, Mohamed Th El-Mohandes, Lubna Mahmoud, A PSO-based multi-objective method for optimal weight factors, placement and sizing of multiple DG units in a distribution system, in: 2019 21st International Middle East Power Systems Conference, MEPCON, IEEE, 2019, pp. 914–920.
[45] Hamid R. Tizhoosh, Opposition-based learning: A new scheme for machine intelligence, in: International Conference on Computational Intelligence for Modelling, Control and Automation and International Conference on Intelligent Agents, Web Technologies and Internet Commerce, CIMCA-IAWTIC'06, vol. 1, IEEE, 2005, pp. 695–701.
[46] Sneha Sultana, Provas Kumar Roy, Krill herd algorithm for optimal location of distributed generator in radial distribution system, Appl. Soft Comput. 40 (2016) 391–404.
[47] Satish Kumar Injeti, N. Prema Kumar, A novel approach to identify optimal access point and capacity of multiple DGs in a small, medium and large scale radial distribution systems, Int. J. Electr. Power Energy Syst. 45 (1) (2013) 142–151.